Emerging Contaminants 11 (2025) 100478

Contents lists available at ScienceDirect

Emerging Contaminants

journal homepage: www.keaipublishing.com/en/journals/emerging-contaminants

Atomic Force Microscopy (AFM) nanomechanical characterization of micro- and nanoplastics to support environmental investigations in groundwater

Massimiliano Galluzzi [a, b, *], Michele Lancia [c, d, **], Chunmiao Zheng [c, d], Viviana Re [e], Valter Castelvetro [f, g], Shifeng Guo [h], Stefano Viaroli [e]

[a] Laboratory of Inflammation and Vaccines, Shenzhen Institute of Advanced Technology, Chinese Academy of Sciences, Shenzhen, 518055, Guangdong, China
[b] China-Italy Joint Laboratory of Pharmacobiotechnology for Medical Immunomodulation, Shenzhen, 518055, China
[c] Guangdong Provincial Key Laboratory of Soil and Groundwater Pollution Control, School of Environmental Science and Engineering, Southern University of Science and Technology, Shenzhen, China
[d] Eastern Institute for Advanced Studies, Eastern Institute of Technology, Ningbo, China
[e] Department of Earth Sciences, University of Pisa, Pisa, Italy
[f] Department of Chemistry and Industrial Chemistry, University of Pisa, Pisa, Italy
[g] CISUP - Center for the Integration of Scientific Instruments of the University of Pisa, University of Pisa, Pisa, Italy
[h] Shenzhen Key Laboratory of Smart Sensing and Intelligent Systems, Shenzhen Institute of Advanced Technology, Chinese Academy of Sciences, Shenzhen, 518055, Guangdong, China

ARTICLE INFO

Article history:
Received 23 November 2024
Received in revised form
26 January 2025
Accepted 2 February 2025
Available online 3 February 2025

Keywords:
Aquifer
Microplastics
Particle aggregates
Surface roughness
Urban hydrology

ABSTRACT

Micro and nanoplastic (MNP) pollution is a severe environmental issue, posing potential risks to environmental and human health due to the intrinsic toxicity of plastic particles and their capacity to adsorb other pollutants. The diffusion of plastic debris affects all the environmental domains, including groundwater which was erroneously believed to be protected by the porous structure of the soil. Advanced spectroscopic techniques can detect the polymer type and quantify the number of MNP particles but are affected by large uncertainties in case of particles smaller than 10 μm in size and MNP heteroaggregates. To advance in the morphological and mechanical characterization of MNPs, a new protocol based on multifrequency Atomic Force Microscopy (AFM) is proposed with the support of the custom open software "MultiFreq AFMSuite". Reconstituted MNP samples in pristine and aged conditions are used to fine-tune the methodology. Multifrequency AFM allows the detection of MNPs up to the nanometric scale based on elastic modulus assessments. The proposed technique also provides an in-depth analysis of the MNP surface roughness and the morphological characterization of particle aggregates. MNP particles from groundwater samples result in aggregates with a roughness of one to two orders of magnitude higher than the plastic particles aged in the laboratory, suggesting a higher adsorption capacity towards pollutants or other natural compounds. The application of the proposed method can facilitate the characterization of micro-and nanoplastics in groundwater, a resource characterized by large uncertainties in hydrodynamics and pollutant transport.

1. Introduction

Micro and nanoplastic (MNP) pollution has become a worldwide issue due to its detrimental effects on the environment and human health [1,2]. Microplastics embrace synthetic polymer particles that are insoluble in water and have at least one dimension between 1 μm and 1000 μm, while nanoplastics encompass a sub-micrometric size [3]. MNPs enter the environment mainly because of mismanagement and further fragmentation of plastic products

* Corresponding author. Shenzhen Institute of Advanced Technology, Chinese Academy of Sciences, Shenzhen, 518055, Guangdong, China.
** Corresponding author. Eastern Institute for Advanced Studies, Eastern Institute of Technology, Ningbo, China.
E-mail addresses: galluzzi@siat.ac.cn (M. Galluzzi), lancia@eitech.edu.cn (M. Lancia).
Peer review under the responsibility of KeAi Communications Co., Ltd.

https://doi.org/10.1016/j.emcon.2025.100478

and waste [4]. They can be carriers of heavy metals, pesticides, pharmaceuticals, and personal care products, with unpredictable environmental and human health impacts [5]. Pollution adsorption mechanisms depend on the specific properties of polymers and contaminants, and the local environmental conditions [6]. MNPs are also prone to form aggregates due to their electrostatic forces, altering their environmental fate.

MNP pollution has permeated all the environmental domains, with critical persistence and pervasiveness across the entire water cycle [7], including groundwater [8]. Groundwater is vital for human life, offering a buffer against climate variability and droughts, supplying 25 % of all water used for irrigation and half of the freshwater withdrawn for domestic purposes [9]. MNPs can reach the water table and potentially pollute the groundwater resources as demonstrated in research investigating aquifers exploited for drinking use [10–12]. However, despite MNP concentration in groundwater is not as abundant as in seawater or freshwater bodies [13,14], the chance for MNPs to adsorb pollutants is relevant in highly stressed aquifers through urban and agricultural pollution. A longer residence time of the MNPs in the aquifers exposes the particles to friction forces generated during the seepage, potentially increasing fragmentation and surface roughness. Morphological data of MNPs can assess aging and provide supportive information about their capacity to adsorb other pollutants [15]. MNPs exhibit a significant tendency to adsorb antibiotics and other polar contaminants, highlighting their potential role in pollutant transport and bioavailability in natural systems [16–18].

MNPs in water and soils are usually detected and quantified using spectroscopic techniques like Raman spectroscopy, Fourier Transform Infrared spectroscopy (FTIR), and Laser Direct Infrared (LDIR). These methods are useful as they allow identifying polymer types by comparing the spectra with vast databases [19], but may be inaccurate in the case of hetero-aggregates, because of the superposition of the spectra of each component [20]. Scanning electron microscope (SEM) analyzes the surface of the fragments down to a nanometric resolution but has large uncertainties in quantifying the fragment surface roughness [21]. Despite their continuous advancements [22], these techniques can hardly allow a detailed characterization of the surface roughness and a three-dimensional reconstruction of the MNP morphology.

In groundwater, MNPs are dragged by the subsoil flow and interact with soil grains. The size of soil pores and throats can be smaller than 10 μm [23], the common detection threshold of spectroscopic methods. Thus, during the seepage at the catchment scale, the soil can retain the larger particles making the MNP detection challenging [24].

Atomic Force Microscopy (AFM) holds significant potential for enhancing the characterization of MNP morphology up to the nanoscale [25], with promising applications in groundwater studies. AFM setup consists of a nanometric probe mounted on a cantilever interacting with the sample surface. The technique produces atomically resolved morphological images together with the spatial distribution of the elastic modulus [26]. Among the different AFM techniques, Multifrequency AFM approaches the sample with a high frequency intermittent force and is appropriate for nanomechanical analyses of particles [27]. Unlike conventional spectroscopic techniques, the proposed multifrequency AFM method provides nanoscale resolution for morphological and mechanical characterization, enabling the detection of MNPs smaller than 10 μm. Additionally, AFM offers quantitative measurements of surface roughness and elastic modulus, which are critical for understanding the aging and interaction dynamics of MNPs. This males AFM nanomechanics a valuable integration to traditional techniques currently used for MNPs assessment.

In this work, AFM is tested on reconstituted samples of pristine to aged plastic fragments because aging processes strongly increase the adsorption capacity of MNPs and progressively alter their mechanical properties [28]. The detection capacity of multifrequency AFM is improved by colocalizing the MNPs with optical fluorescence microscopy combined with a staining agent. The observation of fragment morphology and aggregates is supported in parallel via laser confocal scanning microscopy (LCSM).

Reconstituted MNPs are mixed with clays and chitins to test the AFM detection capacity if MNPs are mixed with organic and inorganic particles commonly found in groundwater. Clay minerals are commonly suspended solids in natural water samples, prone to create aggregates with MNPs due to electrostatic interactions [29]. Chitins are hydrophobic biopolymeric fragments found as degradation debris from insects and crustaceans [30], potentially representing false positives during colocalization with optical fluorescence microscopy. After testing the methodology on reconstituted samples, the proposed technique is applied to two groundwater samples from urban aquifers.

This methodology aims to assess the three-dimensional morphology and surface mechanical properties of MNP fragments and aggregates to support spectroscopic analytical techniques, support the analysis of particle aging, and reconstruct the MNP dynamics in aquifers.

2. Materials and methods

2.1. Materials

Macroscopic and microscopic fragments of polyethylene terephthalate (PET), polyvinyl chloride (PVC), polyamide-6 (PA6), and polyolefin elastomer (POE) were obtained from virgin polymer granules (Sinopec plastic, Shenzhen, China) and used as reference polymers in the preliminary tests. Polystyrene (PS) microspheres, 0.5 μm in size, aqueous dispersion with 2.5 % concentration, were produced by Maikexin Science and Technology (Dongguan, China); PVC microspheres, 1 μm in size and 0.01 % concentration, from Zichuan Technology (Suzhou, China). Polydimethylsiloxane (PDMS) films with a pre-calibrated elastic modulus (2.5 MPa and 3.5 MPa) and PS film at 3.2 GPa were bought from Bruker (Berlin, Germany).

Kaolin clay was purchased from Fuchen (Tianjin, China); illite, montmorillonite, and sodium bentonite from Donghai Construction (Shijiazhuang, China); grounded chitin carapaces of fresh shrimps (*Caridea*) from a local fish market (Guangdong, China); the lipophilic fluorescent dye Nile Red used as the staining agent from Invitrogen (Fisher Scientific, Leics, UK). Cleaved mica, a standard substrate in AFM analyses was retrieved from Ted Pella (Altadena, CA, USA).

2.2. Preparation of reconstituted samples

Microscopic plastic fragments were obtained by grinding and filtering plastic granules in MilliQ water (Direct Q-8 Merck, Rahway, USA), with an average concentration of 0.3 μg/mL. The solution was deposited on cleaved mica and evaporated using a vacuum drying oven (GR-30 Boxun, Shanghai, China) at 60 °C with pressure <0.04 bar for 12 h. Mixtures of grounded MNPs, plastic microspheres, chitins, and clays were prepared using the same protocol, with a 1:1:1 wt ratio. Microspheres underwent a UV accelerated aging in a Dark Box UV Analyzer (model ZF-20D, Gongyi Zihua Instrument, Gongyi, China) for 2 weeks with an average concentration of 0.2 mg/mL in MilliQ water, using 365 nm wavelength at 24 W radiation power.

To guarantee the colocalization of plastic fragments via multifrequency AFM and optical fluorescence microscopy, a staining solution by dissolving Nile red in methanol at 300 μg/mL with a

1:10 dilution was prepared and mixed with the reconstituted sample for 2 min. The final solution was deposited on a gridded glass coverslips Grid-50μm (Ibidi, Gräfelfing, Germany), or a 3.5 cm glass slide for colocalization. The sample was dried in the oven for 12 h.

2.3. Groundwater samples

The two groundwater samples are representative of urban and sub-urban aquifers of Shenzhen (Guangdong, China), a megacity located at the estuary of the Pearl River Delta (Fig. 1a). Shenzhen has 14 million residents and a sub-tropical climate with an average rainfall rate of 2000 mm/y. The local aquifer consists of marine to alluvial sequences interdigitated with laterite soils, lying on crystalline bedrock with low hydraulic conductivity [31].

Sample 1 (Fig. 1b) was obtained from a monitoring well with PVC casing (depth of 16 m) drilled in an alternation of silty sands and clays; Sample 2 from a mountain water spring recharged by the laterite aquifer [31]. During sampling activities, potential cross-contamination was avoided by refraining fixtures with plastic components and synthetic clothes. A stainless-steel bailer with a volume of 1 L was used to collect groundwater from the monitoring well (Sample 1). Groundwater was stored in 1 L glass bottles, previously rinsed with MilliQ water. The bottle opening was protected with aluminum foil sheets. Cross-contamination from the atmospheric fallout was mitigated by piercing the protective aluminum foil sheet of the bottle with the bailer faucet and transferring the water with a laminar flow. A 100 mL glass syringe (Wuxing, Changzhou, China) was used to sample the spring water (Sample 2), respecting the same precautions.

Collected groundwater (100 mL) was filtered with a 0.45 μm cellulose membrane (APS Water Services, Van Nuys, USA) in the laboratory. The filter was rewashed in a 5 mL solution that later was mixed with 5 mL of HCl 36 % for 30 min at room temperature. This treatment did not alter the MNPs but solubilized most of the inorganic particles reducing the interference between particles and the AFM probe. After the staining protocol, the solution was filtered again to collect the residual particles for the AFM analysis. For each step of the described procedure, a blank control sample averted MNP contaminations potentially introduced during the sample preparation.

2.4. AFM and colocalized microscopy setup

AFM setup consists of a nanometric probe mounted on a cantilever interacting with the sample (Fig. 2a). AFM techniques comprehend the quasi-static AFM and the multifrequency AFM. Quasi-static AFM (Fig. 2b) is the most used approach but is not suitable for the nanomechanical characterization of micro to nanometric particles because lateral displacements can occur during force application [32]. On the contrary, multifrequency AFM (Fig. 2c) approaches the sample by applying a high frequency intermittent force and is more appropriate for MNP investigations [27].

The application of multifrequency AFM on MNPs is an innovative topic scarcely investigated in literature. To validate the multifrequency AFM technique on MNPs, a preliminary comparison between quasi-static AFM and multifrequency AFM is performed on macroscopic fragments of plastics and chitins (Figs. S1 and S2). During the interaction between probe and sample, AFM detects forces and indentations with typical precisions of 10^{-12} N and 0.1 nm, respectively. Quasi-static AFM provides the force versus indentation curve, estimating the elastic properties at the nanoscale. The probe exerts a force and simultaneously registers a vertical indentation by approaching the sample vertically. A regular matrix of points reconstructs the local mechanical response of the sample. Specifics of the AFM in quasi-static mode are included in the Supplementary Materials.

Multifrequency AFM measurements utilize a probe-to-sample interaction with a multi-harmonic approach. This approach consists of a bimodal tapping mode (first oscillation mode is amplitude-locked and second mode is frequency-locked) that allows the simultaneous reconstruction of the morphology and the elastic modulus, respectively. Multifrequency AFM minimizes the lateral forces and associated artifacts generated by a strong sample-probe interaction. For small indentation, the calibration of the probe shape is fundamental for quantification but problematic without a well-calibrated surface [33]. Specifics of the AFM in multifrequency mode are included in the Supplementary Materials. Data interpretation is supported by the "MultiFreq AFMsuite" software, compiled on purpose for these experiments (Computer codes and models). Using this software, data can be imported from different AFM producers, and simultaneously visualize maps, masks, histograms and resonance peaks for quantification.

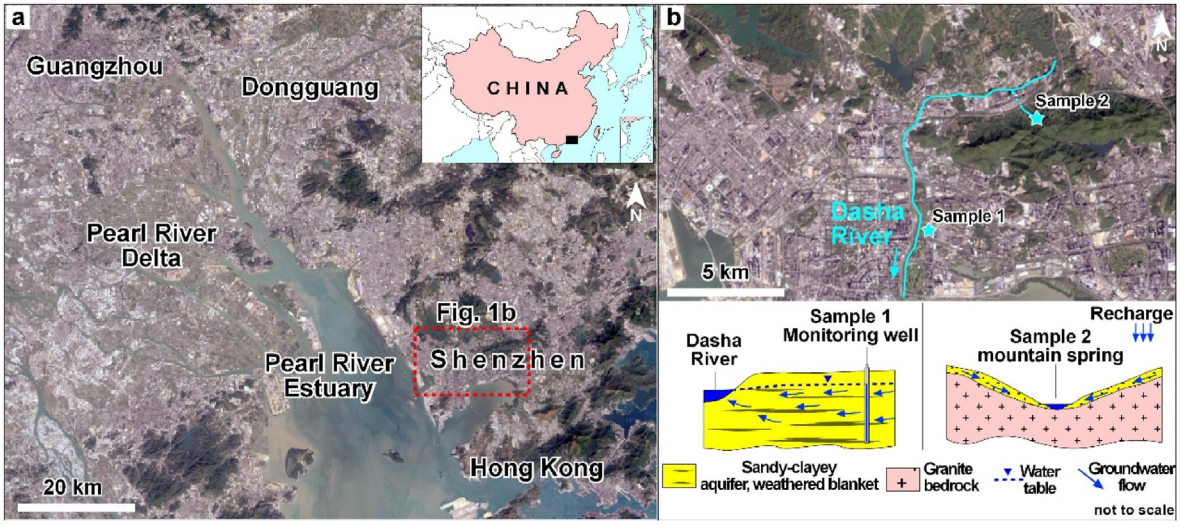

Fig. 1. Satellite image of Pearl River Delta, Southern China (a), the locations of groundwater samples with a simplified groundwater circulation scheme (b).

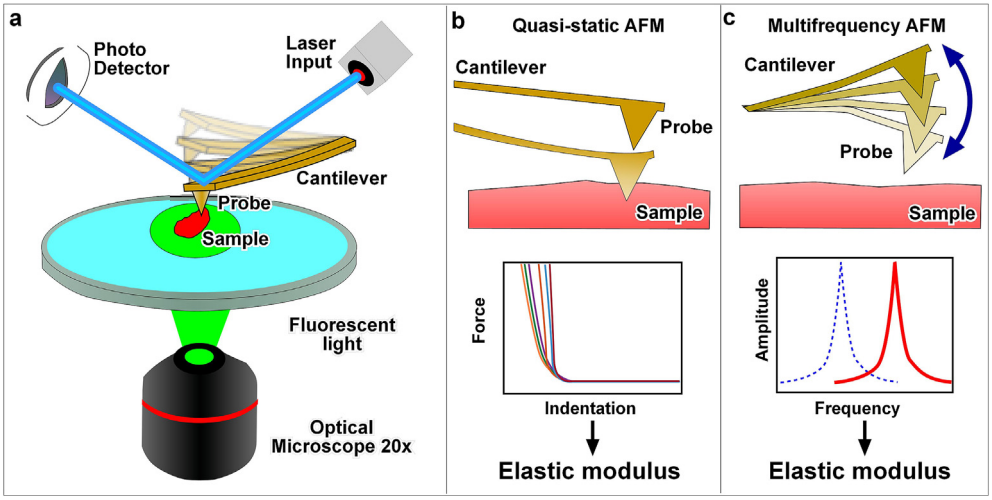

Fig. 2. AFM setup with optical fluorescence co-localization (a); in Quasi-static AFM mode the elastic modulus is measured by the force vs. sample indentation assessment (b); in multifrequency AFM mode by the shift of frequency of second mode resonance (c).

Colocalization experiments between optical fluorescence and AFM (Fig. 2a) were performed on the MFP3Dbio AFM (Asylum Research, Santa Barbara, USA) mounted on an inverted optical microscope (Eclipse Ti2, Nikon, Tokyo, Japan). Mercury lamp (Nikon) and green filter excited the staining agent during the AFM experiments. Optical outputs were recorded with a color-sensitive DS-Fi3 camera (Nikon). MNPs after staining were also observed by laser confocal scanning microscopy (LCSM, A1R, Nikon). Experiments were performed by acquiring transmission and standard TRITC (tetramethyl rhodamine isothiocyanate) fluorescent optical path (excitation: 532 nm, emission: 576 nm) for Nile red fluorescence.

3. Results

3.1. Nanomechanics of reconstituted samples

After deposition on glass or mica substrates, the reconstituted plastic samples are investigated with the multifrequency AFM. AFM quantification is exact if probe geometry is calibrated on a surface with a well-known elastic modulus and near the target of the investigation [33]. Besides plastic fragments, materials with unknown elastic modulus such as chitins and clays were used. Thus, mica and glass substrates were chosen as benchmarks. While this process can allow distinguishing different materials, benchmarking on hard substrate can lead to overestimating the real modulus in plastics. For this reason, the elastic modulus of the investigated plastic fragments falls within a small range between 3.2 GPa and 8.0 GPa (Table 1). The measurement error associated with the narrow elastic modulus range and aging conditions limits the detection capacity among the polymer types. Measurements of fragment morphology, elastic modulus, and quantification histograms for PET, PVC, and PS spheres are presented in Fig. S3 (Supplementary Materials). The four clayey minerals on the mica substrate (kaolin, illite, montmorillonite, and sodium bentonite) show a higher elastic modulus, ranging between 24.9 GPa and 42.5 GPa. Clays can be distinguished from synthetic polymers by considering the elastic modulus, although they are among the softest minerals. Similarly, chitins have an elastic modulus of 35.4 GPa. The morphology, elastic modulus map, and quantification histogram of clays and chitin are reported in Fig. S4.

The nanomechanical detection capacity of multifrequency AFM via the elastic modulus is further tested using a mixture of PS microspheres and sodium bentonite on a mica substrate. PS microspheres have a round morphology while the bentonite clayey minerals aggregate with an irregular shape and distribution (Fig. 3a). The elastic modulus map (Fig. 3b) and the morphological overlay (Fig. 3c) show a sharp mechanical contrast, evidencing the different elastic properties of the mixture. Because of the non-homogeneous distribution of the particles on the substrate during data analysis, results are filtered with a digital selection mask (Fig. 3d) that mitigates the influence of the substrate on the nanomechanical signature of the analyzed materials. In this experiment, the histogram of the elastic modulus (Fig. 3d) shows three peaks corresponding to mica substrate (76.9 GPa), sodium bentonite (47.8 GPa), and PS microspheres (7.2 GPa).

As MNPs dispersed in the environment are characterized by aged fragments, PVC and PS microspheres are investigated via multifrequency AFM before and after aging. Both PVC and PS microspheres show a decay of the mechanical properties with aging and a progressive roughening of their surface. On PVC, the aging protocol also produces abundant nanoplastic debris dispersed on the mica substrate (Fig. 4a). This is coherent with the evidence that the photo-oxidative degradation of hydrocarbon backbone polymers mainly occurs on the surface layers.

The morphological variation of the PVC and PS microspheres is quantified by analyzing the surface roughness (Fig. 4b). To represent the roughness of a curved surface, a spherical deconvolution algorithm is applied (Supplementary Materials). The embrittlement and internal mechanical stresses cause surface cracks and loss of detached material, as evidenced by the increment of roughness and decrease of elastic modulus. However, the aging protocol does not modify the spherical morphology of the microspheres. Analyses were repeated 6 times, with results invariably indicating that the microsphere shape does not significantly change (Fig. 4c). The aging produces marked defects on the surface, resulting in an increment of roughness of 0.2 nm for the PVC and 0.1 nm for the PS. In these measurements, the roughness might be underestimated because of tip geometry convolution, considering a typical radius of 7 nm. For this reason, comparisons were performed always using the same probe. Most significantly, the elastic properties measured at the surface of the aged spheres are reduced by about 50 %.

In natural samples, MNPs have several shapes and sizes and might be assorted with organic and inorganic materials. The application of multifrequency AFM for MNP detection becomes more challenging passing from reconstituted samples in the

Table 1
Elastic modulus of MNPs, clays, and chitin via multifrequency AFM. The probe shape (radius) was fixed by deducing the modulus of the cleaved mica substrate.[a)] Measurements on a glass substrate. The final measurements derive from the average std with N = 4.

Material	Type	Substrate		Particles	
		Elastic modulus (GPa)	Error (GPa)	Elastic modulus (GPa)	Error (GPa)
PET	Fragments	75.7	4.6	5.83	1.57
PVC	Fragments	79	3.2	8.01	1.78
PVC	Microspheres (size 1.0 μm)	78.2	2.1	7.22	1.09
PVC aged	Microspheres (size 1.0 μm)	76.9	2.3	3.21	0.69
PS	Microspheres (size 0.5 μm)	78.12	2.49	6.78	1.01
PS aged	Microspheres (size 0.5 μm)	80.83	2.67	4.95	0.99
Kaolin Clay	Powder (Bulk)	81.08	0.75	24.9	2.68
Illite Clay	Powder (Bulk)	82.1	1.8	25	1.9
Montmorillonite Clay	Powder (Bulk)	79.6	0.5	42.4	4.8
Sodium Bentonite Clay	Powder (Bulk)	81.9	3.3	29.9	3.2
Chitin[a)]	Fragments	60.5	4.7	35.4	2.1

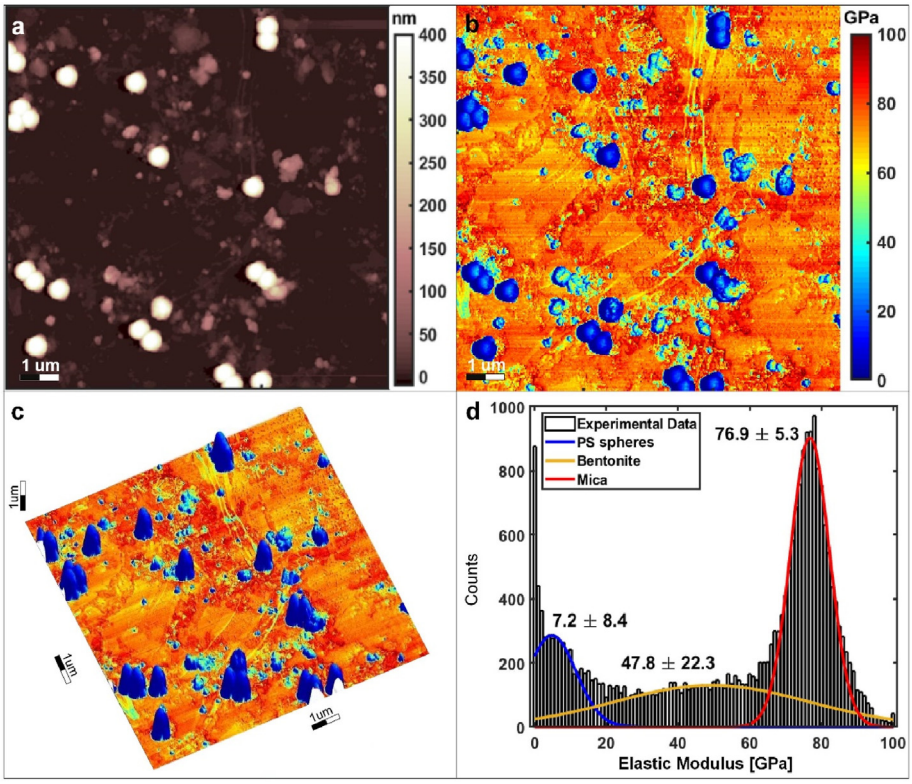

Fig. 3. Co-deposition of PS microspheres mixed with sodium bentonite on mica substrate: morphology map (a), elastic modulus map (b), overlay of elastic modulus colors on three-dimensional morphology (c); histogram chart showing Gaussian fit for different materials (d), labels indicate the elastic modulus (GPa).

laboratory to natural samples such as groundwater. Using the Nile Red staining agent from Invitrogen (Fisher Scientific, Leics, UK), the MNP detection capacity is strengthened by taking advantage of the hydrophobicity of the plastic particles, regardless of their aging conditions. Results of the staining protocol on a mixture of ground PVC fragments, clays, and chitins are presented (Fig. S5). The observation of fragment morphology via LCSM confirms that microplastics can be distinguished from chitins thanks to a fluorescence intensity three times higher. After staining, clays are not sensitive to fluorescent light (Fig. S5).

3.2. MNPs in groundwater

The MNP fragments from the two groundwater samples collected in urban aquifers (Sample 1 and Sample 2) are markedly different in morphology and roughness from the reconstituted samples as the friction forces and aging processes occurring in the environment are more intense. To show the potentiality of the MNP detection, an aggregate from Sample 1 is characterized via multifrequency AFM and optical fluorescence microscopy colocalization (Fig. 5a). The MNPs are sensitive to fluorescent light with an intensity five times higher (Fig. 5b) than the agglomerates of the staining agent (needle-shaped). A multifrequency AFM analysis is carried out on a selected portion (the red square of Fig. 5a, size 10 μm × 10 μm). Both morphology (Fig. 5c) and elastic modulus (Fig. 5d) maps testify that the fluorescent particle is an aggregate composed of sub-micrometric fragments of plastic. After a surface deconvolution on a restricted area of 1 μm^2, the average roughness results about 45 nm, indicating a strong surface degradation and cracking. The quantification histogram of the analyzed fragments assesses an average elastic modulus of about 7.5 GPa (Fig. S6). Sparse nanometric plastic fragments are visible in the left bottom

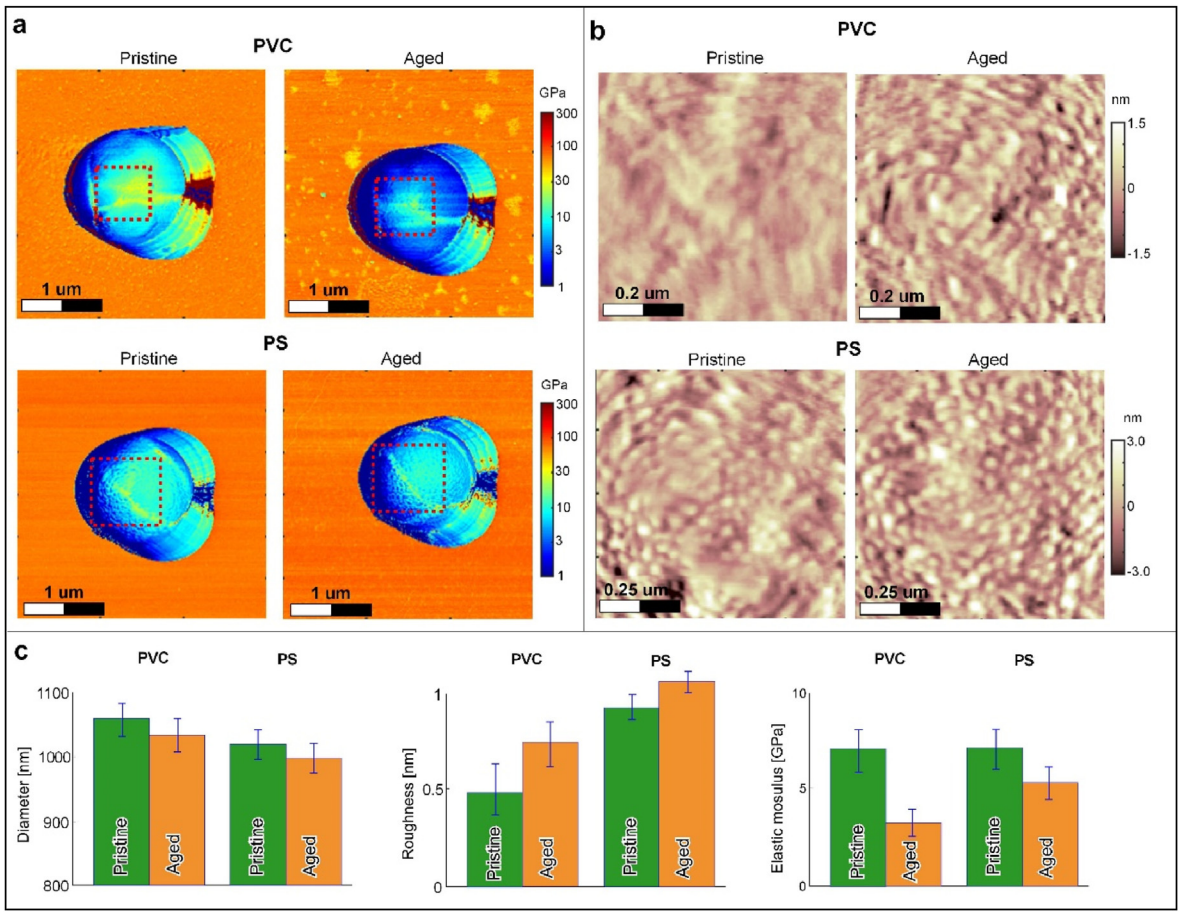

Fig. 4. Elastic modulus map of PVC and PS microspheres before and after the aging (a); surface close-up after spherical deconvolution of pristine and aged microspheres (b); diameter, elastic modulus, and roughness of pristine and aged microspheres (c).

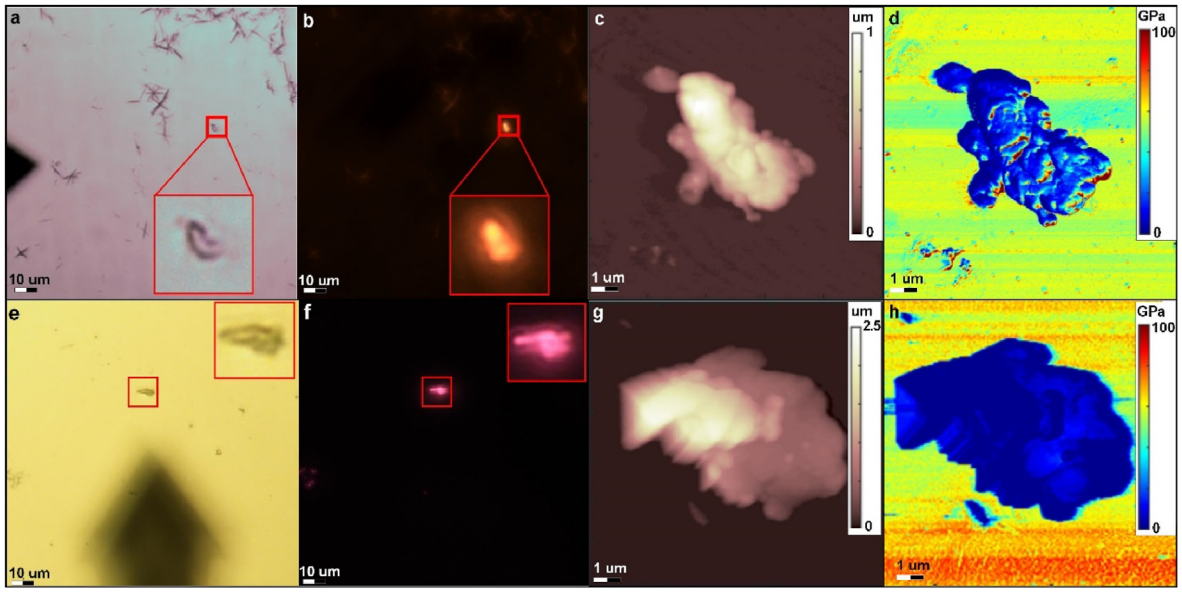

Fig. 5. Colocalization of a plastic fragment from groundwater samples 1 and 2. Sample 1: optical transmission image (a); fluorescence signal from green light (b); AFM morphology of the red box (c); and elastic modulus map (d). Sample 2: optical transmission image (e); fluorescence signal from green light (f); AFM morphology of the red box (g); and elastic modulus map (h).

corner (Fig. 5d), and show a similar elastic modulus, with a vertical-to-horizontal ratio of 0.1. These fragments were not previously detected by optical fluorescence microscopy due to their exiguous size. Other clasts and aggregates, characterized by a similar morphology and roughness, are detected but not presented.

MNPs are also detected in groundwater Sample 2 (Fig. 5e). Results of a fragment with high-intensity fluorescence are proposed (Fig. 5f). Multifrequency AFM morphology and elastic modulus maps reconstruct a single plastic fragment with aggregates on top (Fig. 5g). AFM identifies small nanometric particles around the main body with the same mechanical properties but not visible by optical fluorescence microscopy (Fig. 5h). The quantification histogram of the analyzed fragment assesses an average elastic modulus of about 7.5 GPa (Fig. S6). After a surface deconvolution and restriction on a 1 μm^2 area, the local roughness results in about 4 nm, indicating a noticeable surface degradation. Other fragments and aggregates, characterized by a similar morphology and roughness, are detected but not characterized.

4. Discussions

Results of the analyses via multifrequency AFM suggest that the elastic modulus range can be used to distinguish the MNPs from other materials commonly found in groundwater samples. Compared to spectroscopic methods focused on polymer type, the multifrequency AFM is invaluable in the three-dimensional characterization of the MNPs, including the roughness quantification at the nanometric scale. The proposed approach can characterize nanoplastics aggregates that represent an open challenge even in the most advanced spectroscopic analyses [20]. The polymer degradation processes caused by environmental aging, that for carbon chain polymers such as polystyrene is mainly the result of photooxidation induced by UV exposure upon solar irradiation. This results in alterations not only of the polymer's chemical structure, but also of the particle's surface morphology, with significant increase of the active surface area of MNPs. This increase is fundamentally correlated with the enhanced roughness observed at the nanoscale, as quantified through AFM. The chemical alterations caused by photooxidative aging involve chain scissions and oxidations, the latter contributing to the particle's surface change. These combined effects, greater surface roughness and altered surface chemistry, enhance the adsorption capacity of aged MNPs. In addition, the multifrequency AFM can contribute to the MNP characterization, supporting a deeper understanding of MNP contamination assessments in the aquifer. MNP circulation is limited by the pore throats of the subsoil that filter the MNP particles. A systematic analysis of the MNP aggregates via the multifrequency AFM can provide essential information on the filtration capacity of the aquifer at the catchment scale. The aggregates can originate via the agglomeration of MNP particles at the sampling sites such as in the water well casing. Aggregate formation during the sample treatment such as the filtration is not excluded.

In the analyzed groundwater samples, the occurrence of aggregates made of particles smaller than the detection threshold of the spectroscopic techniques is confirmed. Aggregates are made of MNP fragments with a size of 1 μm−5 μm, consistent with the predicted size pore size of sandy soils [23].

Multifrequency AFM cannot recognize the polymer type, but it can quantify the morphological effects of the aging processes these particles underwent. The occurrence of aggregates made of submicrometric fragments is coherent with the sorting and filtering action operated by the soil during the seepage processes. In the urban context of Sample 1, the detected MNPs may originate from the urban recharge [34], and the atmospheric fallout. However, the degradation of the PVC casing of the monitoring well might be an additional source of pollution [35]. The catchment of Sample 2 is located in a mountain area, and the source of MNPs is probably the atmospheric fallout. The degradation of unmanaged plastic waste is irrelevant thanks to the rural land use and the dense tropical vegetation. MNPs are introduced in the shallow aquifers thanks to the infiltration of the abundant rainfall and are slowly transported through the aquifer toward the water wells and springs (Fig. 6). The average roughness range of detected aggregates, between 4 nm and 45 nm, is higher than in the pristine and artificially aged microspheres from reconstituted samples. This could result from longer and more intense aging processes in the natural environment.

This study primarily focuses on groundwater due to its relatively low contaminant load in the case of microplastics, which simplifies sample preparation, and the nanoscale sensitivity of the AFM methodology, making it ideal for detecting MNPs. These contaminants can also be investigated via AFM on other environmental matrices, including soil, marine and other surface waters, living organisms and airborne particulate. These applications would necessitate tailored pretreatment protocols to address challenges such as organic matter, high particulate loads, and mineral interference.

4.1. Limits, uncertainties and prospectives

Based on counting and characterization of the polymer type, the spectroscopic methods are inescapable for a fast characterization of

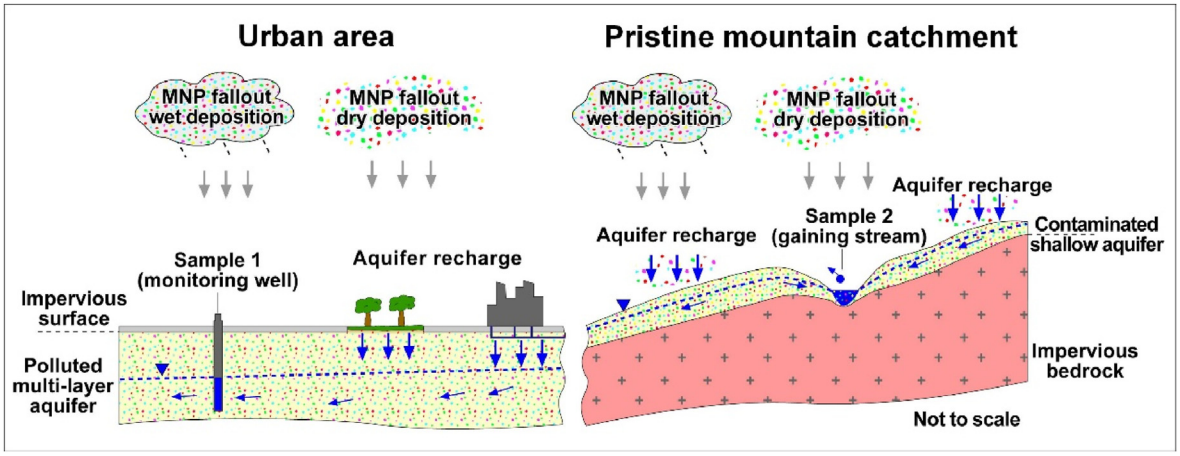

Fig. 6. The MNPs dynamics in urban aquifers and mountain catchment.

the MNPs. The multifrequency AFM approach is specifically used to add invaluable information on particle geometry and structure, minimizing the influence on nanoparticle displacement. Unfortunately, the errors due to the irregular contact geometry between the AFM probe and the microscopic fragment do not allow a distinction among polymers. In fact, the mechanical contact model is built on the geometry of a sphere or cone indenting an ideally flat surface. When the indentation is smaller or roughness is comparable with the indentation, the AFM probe is sensitive to asperities, deviating from the flat surface. In correspondence with cavities, the probe has a higher contact surface, resulting in an overestimation of the elastic modulus, eventually increasing the uncertainty of its quantification.

The mechanical AFM method in its current form is primarily designed for nanomechanical and morphological characterization, with limited capability for polymer type identification. However, coupling AFM and spectroscopic methodologies such as AFM-IR or Tip-Enhanced Raman Spectroscopy (TERS) are promising options to overcome this limitation, with the potential to provide a comprehensive characterization of MNPs down to nanoscale. For instance, AFM-IR uses an atomic force tip and infrared laser excitation to record high-resolution topography and chemical spectra. This technique allowed to successfully characterize PS spheres as small as 20 nm in aqueous environment [36]. TERS was successfully used to characterize the surface composition of a thin film of a polyisoprene/polystyrene blend [37]. While these combined instruments are rare and expensive, they may represent a potential future direction for expanding AFM-based methodologies into environmental studies on MNPs, and in particular on the more elusive nanoplastics.

5. Conclusions

Multifrequency AFM successfully detects the MNPs and provides unique information about their roughness and morphology in natural samples such as groundwater, both on single fragments and aggregates, representing an advancement in the characterization of the aging processes of MNPs. Aggregates are typically characterized by a surface area larger than entire particles of comparable size, indicative of a later stage of degradation and higher adsorption capacity. Therefore, they likely have a higher potential toxicity than fragments detected by standard spectroscopic methods, due to enhanced interactions with other environmental pollutants and living organisms. The proposed protocol can successfully support traditional and advanced spectroscopic techniques, more effective in fragment counting and detection of the polymer type. Despite the absence of polymer identification, the proposed AFM methodology is widely applicable with basic instrumentation, offering a cost-effective solution to measure surface roughness, morphology, and mechanical properties of MNPs. The overall protocol fills a critical gap, particularly for the characterization of particles smaller than 10 μm, where conventional spectroscopic methods face significant uncertainties.

This combined approach is invaluable in groundwater studies, where MNPs are aggregated and interact with soil that operates a sorting of MNP particles. The pronounced aging of the investigated fragments is likely associated with increased toxicity. The systematic study of the roughness and morphology of MNPs in groundwater can further help characterize the contaminant source as the residence time.

CRediT authorship contribution statement

Massimiliano Galluzzi: Writing – original draft, Software, Funding acquisition, Conceptualization. **Michele Lancia:** Writing – original draft, Visualization, Methodology, Data curation. **Chunmiao Zheng:** Writing – review & editing, Supervision, Funding acquisition. **Viviana Re:** Writing – review & editing, Validation. **Valter Castelvetro:** Writing – review & editing, Supervision, Resources, Funding acquisition. **Shifeng Guo:** Writing – review & editing, Validation. **Stefano Viaroli:** Writing – review & editing, Validation.

Computer code and models

The software “MultiFreq AFMSuite” and manual are freely available in an open repository: https://github.com/marsdeck/MultiFreq-Suite.

Data availability

All the datasets are available upon request to the corresponding authors.

Declaration of competing interest

The authors declare that they have no known competing financial interests or personal relationships that could have appeared to influence the work reported in this paper.

Acknowledgments

This work was supported by the National Key R&D Program of China (2023YFE0117000), the Italian Ministry of Foreign Affairs and International Cooperation (PGR02013) – ENCOMPASS, the National Natural Science Foundation of China (Grant No. 32071318, 52071332, T2350610283), the Guangdong Basic and Applied Basic Research Foundation (Grant No. 2024A1515012508), the Youth Innovation Promotion Association of the Chinese Academy of Sciences (Grant No. 2022363), and the European Union's Horizon 2020 research and innovation program under the Marie Skłodowska-Curie Actions Grant (101028018) - SPONGE funded by European Commission.

Appendix A. Supplementary data

Supplementary data to this article can be found online at https://doi.org/10.1016/j.emcon.2025.100478.

References

[1] L. Li, Y. Luo, R. Li, Q. Zhou, W.J.G.M. Peijnenburg, N. Yin, J. Yang, C. Tu, Y. Zhang, Effective uptake of submicrometre plastics by crop plants via a crack-entry mode, Nat. Sustain. 3 (2020) 929–937, https://doi.org/10.1038/s41893-020-0567-9.
[2] A. Sun, W.-X. Wang, Human exposure to microplastics and its associated health risks, Environ. Health 1 (2023) 139–149, https://doi.org/10.1021/envhealth.3c00053.
[3] ISO, International Organization for Standardization, Principles for the analysis of microplastics present in the environment. https://www.iso.org/standard/78033.html, 2023.
[4] J.P.G.L. Frias, R. Nash, Microplastics: finding a consensus on the definition, Mar. Pollut. Bull. 138 (2019) 145–147, https://doi.org/10.1016/j.marpolbul.2018.11.022.
[5] N. Rafa, B. Ahmed, F. Zohora, J. Bakya, S. Ahmed, S.F. Ahmed, M. Mofijur, A.A. Chowdhury, F. Almomani, Microplastics as carriers of toxic pollutants: source, transport, and toxicological effects, Environ. Pollut. 343 (2024) 123190, https://doi.org/10.1016/j.envpol.2023.123190.
[6] Y. Changfu, G. Jiani, Y. Yidi, L. Yijin, L. Yiyao, F. Yu, Interface behavior changes of weathered polystyrene with ciprofloxacin in seawater environment, Environ. Res. 212 (2022) 113132, https://doi.org/10.1016/j.envres.2022.113132.
[7] P.S. Ross, S. Chastain, E. Vassilenko, A. Etemadifar, S. Zimmermann, S.-A. Quesnel, J. Eert, E. Solomon, S. Patankar, A.M. Posacka, B. Williams, Pervasive distribution of polyester fibres in the Arctic Ocean is driven by Atlantic inputs, Nat. Commun. 12 (2021) 106, https://doi.org/10.1038/s41467-020-

20347-1.
[8] J.-Y. Lee, J. Jung, M. Raza, Good field practice and hydrogeological knowledge are essential to determine reliable concentrations of microplastics in groundwater, Environ. Pollut. 308 (2022) 119617, https://doi.org/10.1016/j.envpol.2022.119617.
[9] UNESCO, Water for Prosperity and Peace, UN-Water, Paris, France, 2024.
[10] B. Wu, L.-W. Li, Y.-X. Zu, J. Nan, X.-Q. Chen, K. Sun, Z.-L. Li, Microplastics contamination in groundwater of a drinking-water source area, northern China, Environ. Res. 214 (2022) 114048, https://doi.org/10.1016/j.envres.2022.114048.
[11] J. Shi, Y. Dong, Y. Shi, T. Yin, W. He, T. An, Y. Tang, X. Hou, S. Chong, D. Chen, K. Qin, H. Lin, Groundwater antibiotics and microplastics in a drinking-water source area, northern China: occurrence, spatial distribution, risk assessment, and correlation, Environ. Res. 210 (2022) 112855, https://doi.org/10.1016/j.envres.2022.112855.
[12] E. Brancaleone, D. Mattei, V. Fuscoletti, L. Lucentini, G. Favero, G. Cecchini, A. Frugis, V. Gioia, M. Lazzazzara, Microplastic in drinking water: a pilot study, Microplastics 3 (2024) 31–45, https://doi.org/10.3390/microplastics3010003.
[13] V. Re, Shedding light on the invisible: addressing the potential for groundwater contamination by plastic microfibers, Hydrogeol. J. 27 (2019) 2719–2727, https://doi.org/10.1007/s10040-019-01998-x.
[14] G. Chen, Y. Zou, G. Xiong, Y. Wang, W. Zhao, X. Xu, X. Zhu, J. Wu, F. Song, H. Yu, Microplastic transport and ecological risk in coastal intruded aquifers based on a coupled seawater intrusion and microplastic risk assessment model, J. Hazard Mater. 480 (2024) 135996, https://doi.org/10.1016/j.jhazmat.2024.135996.
[15] Z. Ren, X. Gui, X. Xu, L. Zhao, H. Qiu, X. Cao, Microplastics in the soil-groundwater environment: aging, migration, and co-transport of contaminants – a critical review, J. Hazard Mater. 419 (2021) 126455, https://doi.org/10.1016/j.jhazmat.2021.126455.
[16] N. Liu, F. Yu, Y. Wang, J. Ma, Effects of environmental aging on the adsorption behavior of antibiotics from aqueous solutions in microplastic-graphene coexisting systems, Sci. Total Environ. 806 (2022) 150956, https://doi.org/10.1016/j.scitotenv.2021.150956.
[17] P. Liu, L. Qian, H. Wang, X. Zhan, K. Lu, C. Gu, S. Gao, New insights into the aging behavior of microplastics accelerated by advanced oxidation processes, Environ. Sci. Technol. 53 (2019) 3579–3588, https://doi.org/10.1021/acs.est.9b00493.
[18] S. Zhuang, J. Wang, Interaction between antibiotics and microplastics: recent advances and perspective, Sci. Total Environ. 897 (2023) 165414, https://doi.org/10.1016/j.scitotenv.2023.165414.
[19] Y.K. Song, S.H. Hong, S. Eo, W.J. Shim, A comparison of spectroscopic analysis methods for microplastics: manual, semi-automated, and automated Fourier transform infrared and Raman techniques, Mar. Pollut. Bull. 173 (2021) 113101, https://doi.org/10.1016/j.marpolbul.2021.113101.
[20] N. Qian, X. Gao, X. Lang, H. Deng, T.M. Bratu, Q. Chen, P. Stapleton, B. Yan, W. Min, Rapid single-particle chemical imaging of nanoplastics by SRS microscopy, Proc. Natl. Acad. Sci. U.S.A. 121 (2024) e2300582121, https://doi.org/10.1073/pnas.2300582121.
[21] Y. Xiong, J. Zhao, L. Li, Y. Wang, X. Dai, F. Yu, J. Ma, Interfacial interaction between micro/nanoplastics and typical PPCPs and nanoplastics removal via electrosorption from an aqueous solution, Water Res. 184 (2020) 116100, https://doi.org/10.1016/j.watres.2020.116100.
[22] A. Nene, S. Sadeghzade, S. Viaroli, W. Yang, U.P. Uchenna, A. Kandwal, X. Liu, P. Somani, M. Galluzzi, Recent advances and future technologies in nano-microplastics detection, Environ. Sci. Eur. 37 (n.d.). https://doi.org/10.1186/S12302-024-01044-Y.
[23] H. Minagawa, Y. Nishikawa, I. Ikeda, K. Miyazaki, N. Takahara, Y. Sakamoto, T. Komai, H. Narita, Characterization of sand sediment by pore size distribution and permeability using proton nuclear magnetic resonance measurement, J. Geophys. Res. 113 (2008) 2007JB005403, https://doi.org/10.1029/2007JB005403.
[24] S. Viaroli, M. Lancia, V. Re, Microplastics contamination of groundwater: current evidence and future perspectives. A review, Sci. Total Environ. 824 (2022) 153851, https://doi.org/10.1016/j.scitotenv.2022.153851.
[25] Z. Chen, X. Shi, J. Zhang, L. Wu, W. Wei, B.-J. Ni, Nanoplastics are significantly different from microplastics in urban waters, Water Res. X 19 (2023) 100169, https://doi.org/10.1016/j.wroa.2023.100169.
[26] S. Benaglia, V.G. Gisbert, A.P. Perrino, C.A. Amo, R. Garcia, Fast and high-resolution mapping of elastic properties of biomolecules and polymers with bimodal AFM, Nat. Protoc. 13 (2018) 2890–2907, https://doi.org/10.1038/s41596-018-0070-1.
[27] R. Garcia, E.T. Herruzo, The emergence of multifrequency force microscopy, Nat. Nanotechnol. 7 (2012) 217–226, https://doi.org/10.1038/nnano.2012.38.
[28] Z. Zhou, Y. Sun, Y. Wang, F. Yu, J. Ma, Adsorption behavior of Cu(II) and Cr(VI) on aged microplastics in antibiotics-heavy metals coexisting system, Chemosphere 291 (2022) 132794, https://doi.org/10.1016/j.chemosphere.2021.132794.
[29] X. Yang, C. An, Q. Feng, M. Boufadel, W. Ji, Aggregation of microplastics and clay particles in the nearshore environment: characteristics, influencing factors, and implications, Water Res. 224 (2022) 119077, https://doi.org/10.1016/j.watres.2022.119077.
[30] B. Duan, H. Gao, M. He, L. Zhang, Hydrophobic modification on surface of chitin sponges for highly effective separation of oil, ACS Appl. Mater. Interfaces 6 (2014) 19933–19942, https://doi.org/10.1021/am505414y.
[31] M. Lancia, H. Su, Y. Tian, J. Xu, C. Andrews, D.N. Lerner, C. Zheng, Hydrogeology of the Pearl River Delta, southern China, J. Maps 16 (2020) 388–395, https://doi.org/10.1080/17445647.2020.1761903.
[32] H.-J. Butt, B. Cappella, M. Kappl, Force measurements with the atomic force microscope: technique, interpretation and applications, Surf. Sci. Rep. 59 (2005) 1–152, https://doi.org/10.1016/j.surfrep.2005.08.003.
[33] R. Garcia, R. Proksch, Nanomechanical mapping of soft matter by bimodal force microscopy, Eur. Polym. J. 49 (2013) 1897–1906, https://doi.org/10.1016/j.eurpolymj.2013.03.037.
[34] D.N. Lerner, Identifying and quantifying urban recharge: a review, Hydrogeol. J. 10 (2002) 143–152, https://doi.org/10.1007/s10040-001-0177-1.
[35] S. Viaroli, M. Lancia, J.-Y. Lee, Y. Ben, R. Giannecchini, V. Castelvetro, R. Petrini, C. Zheng, V. Re, Limits, challenges, and opportunities of sampling groundwater wells with plastic casings for microplastic investigations, Sci. Total Environ. 946 (2024) 174259, https://doi.org/10.1016/j.scitotenv.2024.174259.
[36] I.C. Ten Have, A.J.A. Duijndam, R. Oord, H.J.M. Van Berlo-van Den Broek, I. Vollmer, B.M. Weckhuysen, F. Meirer, Photoinduced force microscopy as an Efficient method towards the detection of nanoplastics, Chem. Methods 1 (2021) 205–209, https://doi.org/10.1002/cmtd.202100017.
[37] B. Yeo, E. Amstad, T. Schmid, J. Stadler, R. Zenobi, Nanoscale probing of a polymer-blend thin film with tip-enhanced Raman spectroscopy, Small 5 (2009) 952–960, https://doi.org/10.1002/smll.200801101.